

Introduction to HssA test site



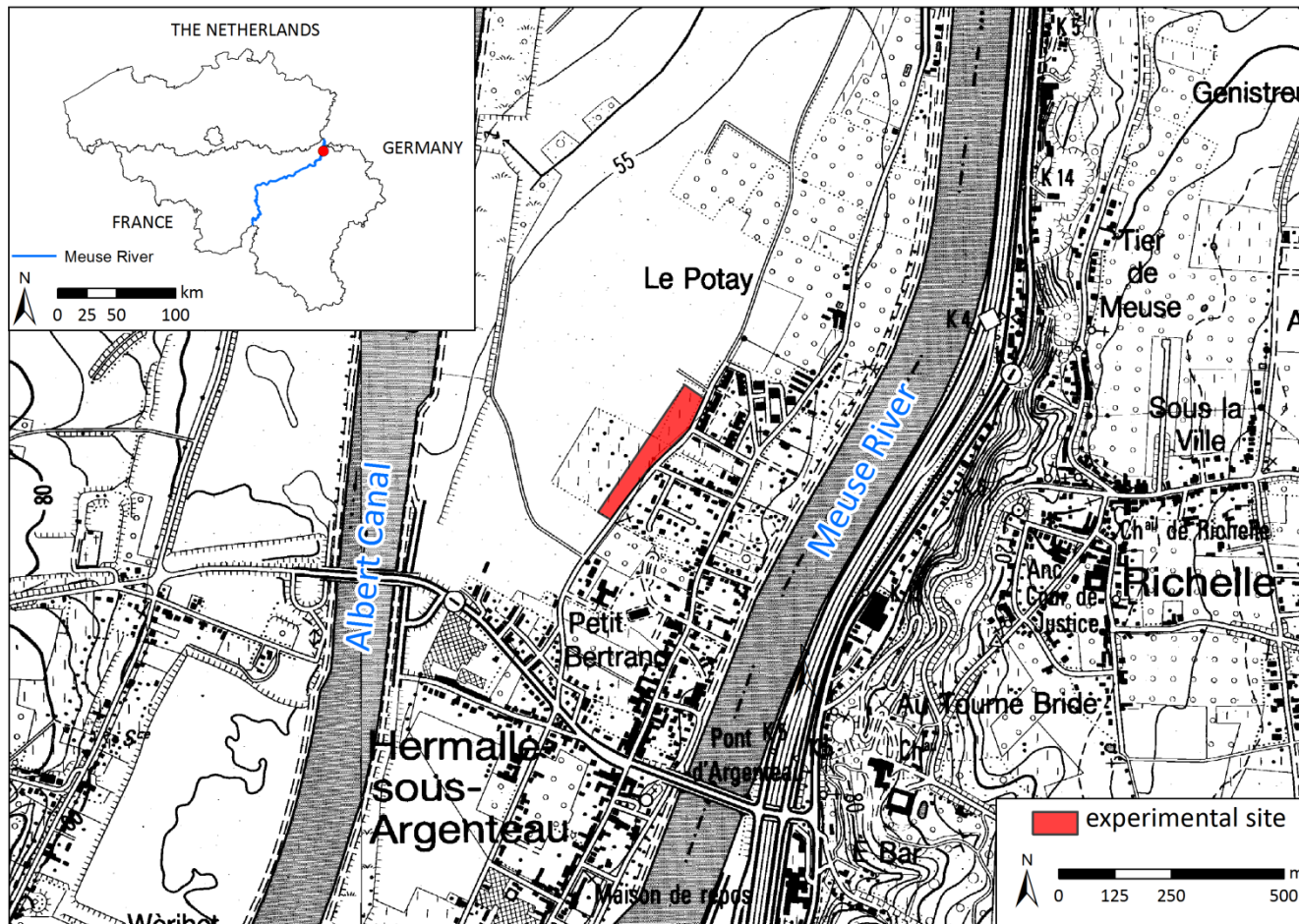
Pierre JAMIN |

12/10/2017



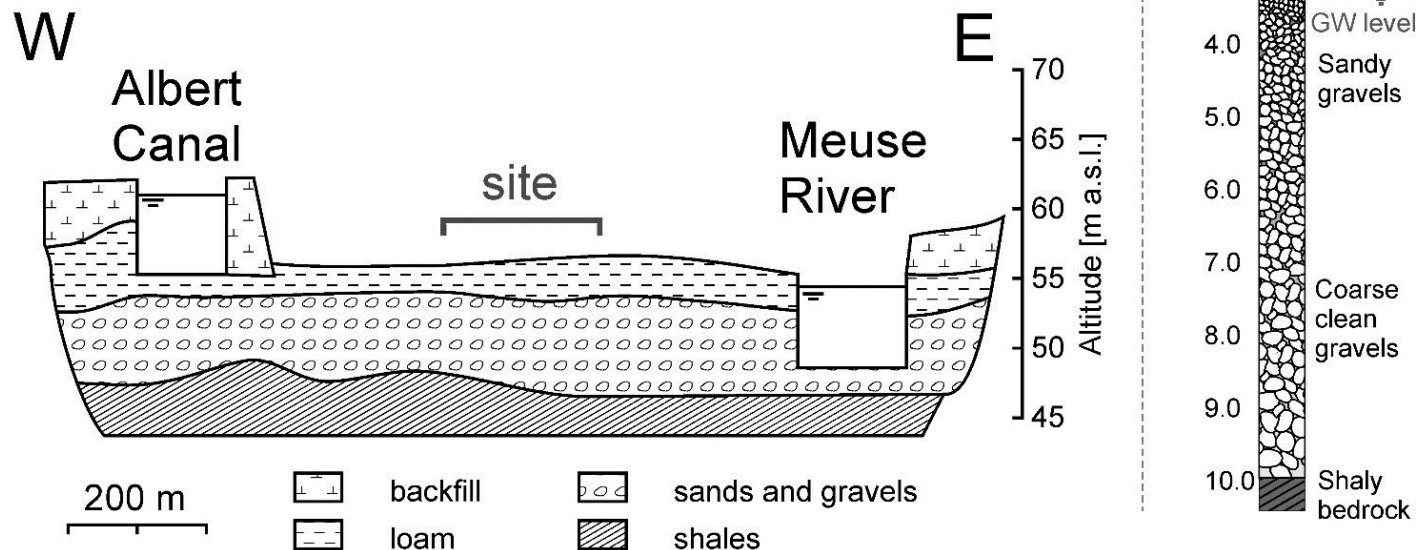
Location : Alluvial plain of the Meuse

- Rue Joseph Bonhomme, Hermalle-sous-Argenteau ($X_{\text{Lambert}}=242670 \text{ m}$, $Y_{\text{Lambert}}=157150 \text{ m}$)
- Between the Albert Canal and the Meuse River



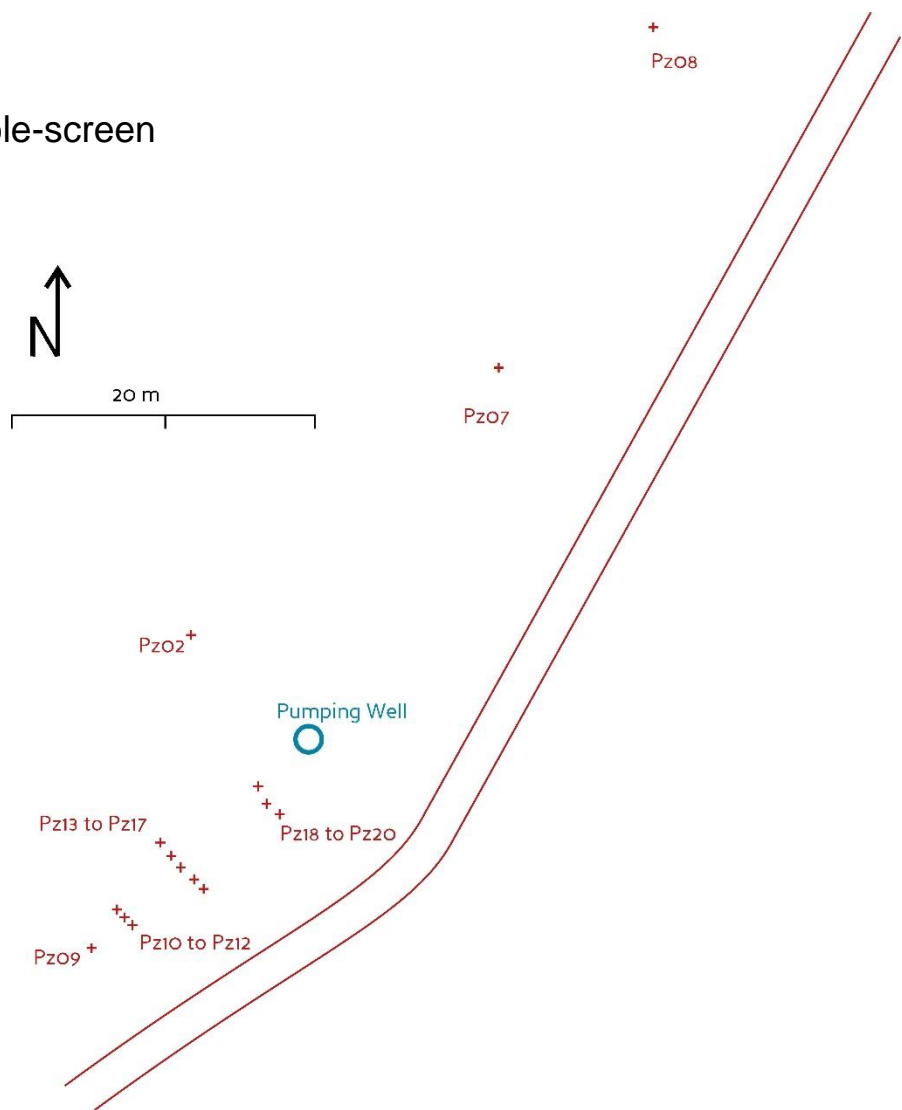
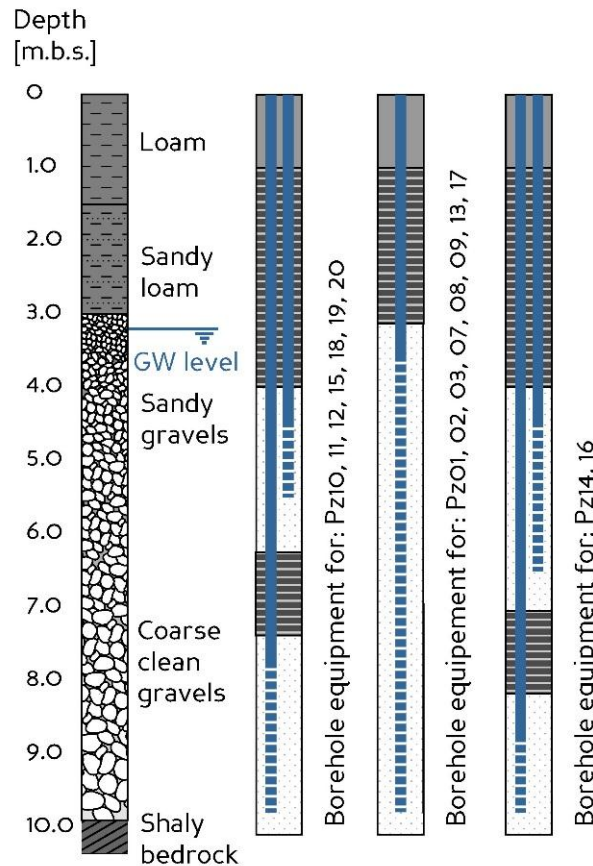
Geology : Alluvial plain sediments

- 3 m of loam
- 7 m of sandy gravels than becomes coarser and cleaner with depth
- Shaly bedrock at 10 m below surface = base of the aquifer
- GW level 3.2 m below surface, unconfined aquifer
- Seasonal variation 0.5 m, high level in january



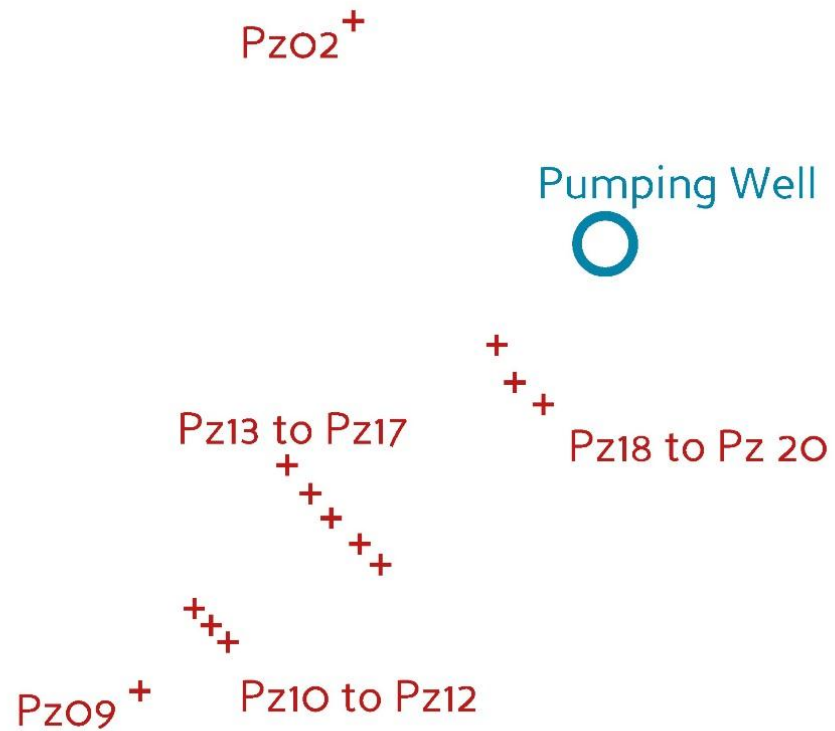
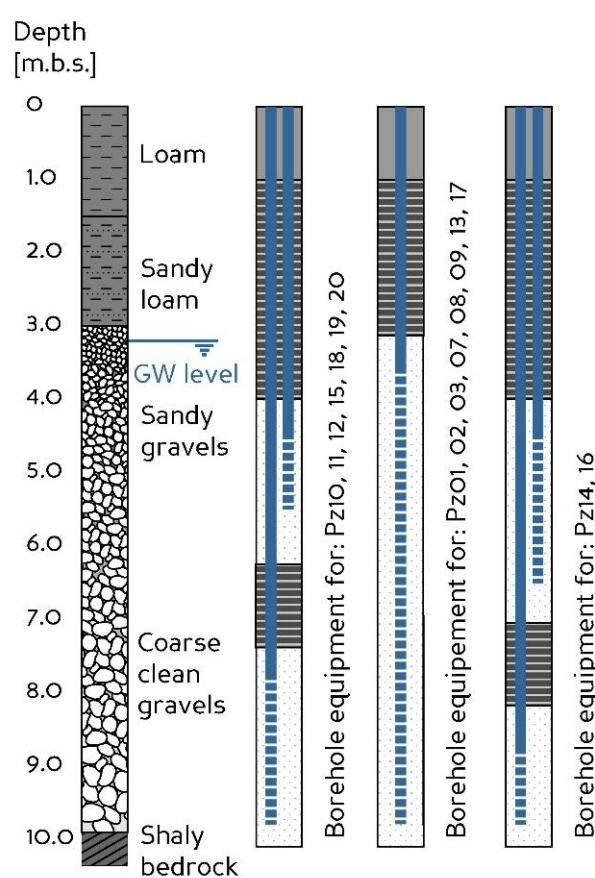
Equipment : 1 Pumping well, 15 piezometers, electricity

- 6" pumping well fully screened
- 3 « old » 2" piezometers fully screened
- 12 « new » 2" piezometers, 3 fully screened, 9 double-screen
- Electricity available on site (3x400V)



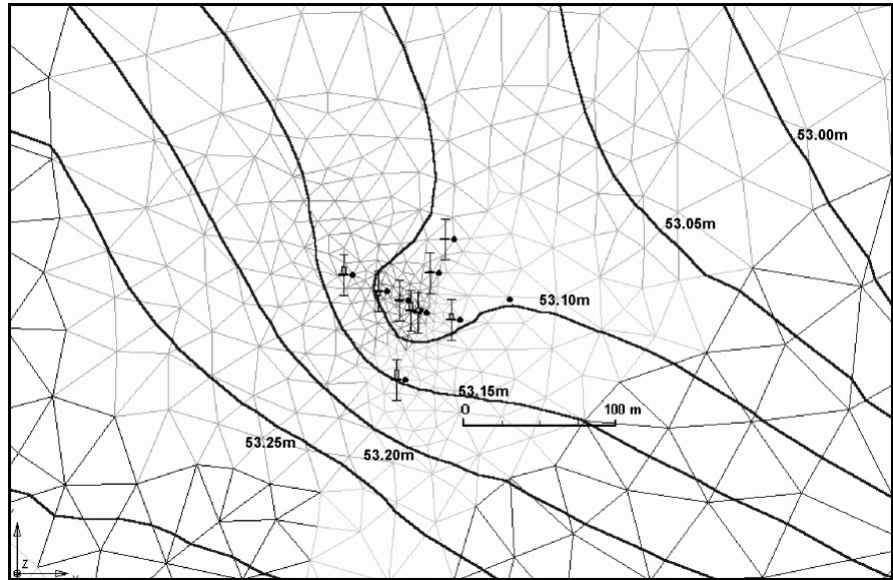
Equipment : 1 Pumping well, 15 piezometers, electricity

- 6" pumping well fully screened
- 3 « old » 2" piezometers fully screened
- 12 « new » 2" piezometers, 3 fully screened, 9 double-screen
- Electricity available on site (3x400V)



First site characterization: 2001 PhD of Brouyère S.

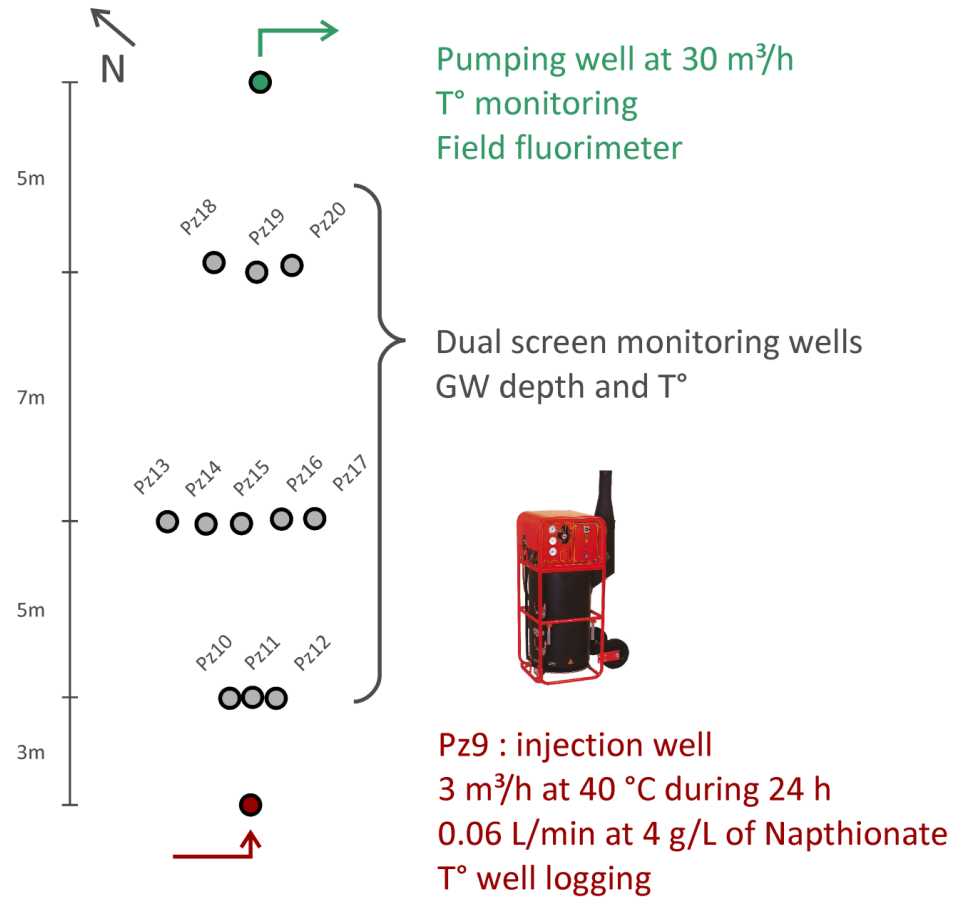
- Pumping tests determining $K = 1,8$ to $7,6 \cdot 10^{-2} \text{ m/s}$
- Hydraulic gradient 0.5 % NE
- Effective porosity 0.04 to 0.08
- Immobile porosity 0.1 to 0.4
- Longitudinal dispersivity 0.5 to 4.5 m
- Tracer behavior on site :
 - I, NO₃, Cl, Br conservative
 - Li, K, Sr, Fluoresceine, Rhodamine can be adsorbed
 - Naphthionate degrades with 1st order coef $1,5 \cdot 10^{-5} \text{ s}^{-1}$
- Modeling



2012 Thermal tracer test: Heat + Naphtionate

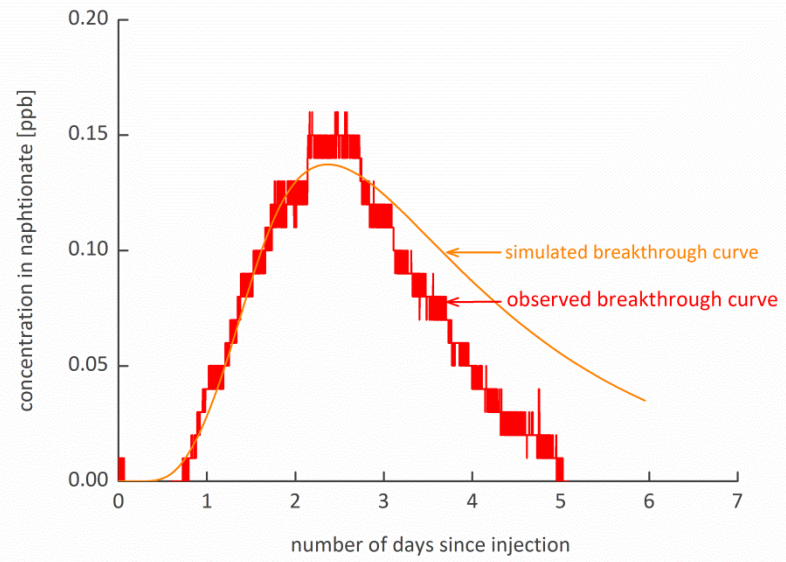
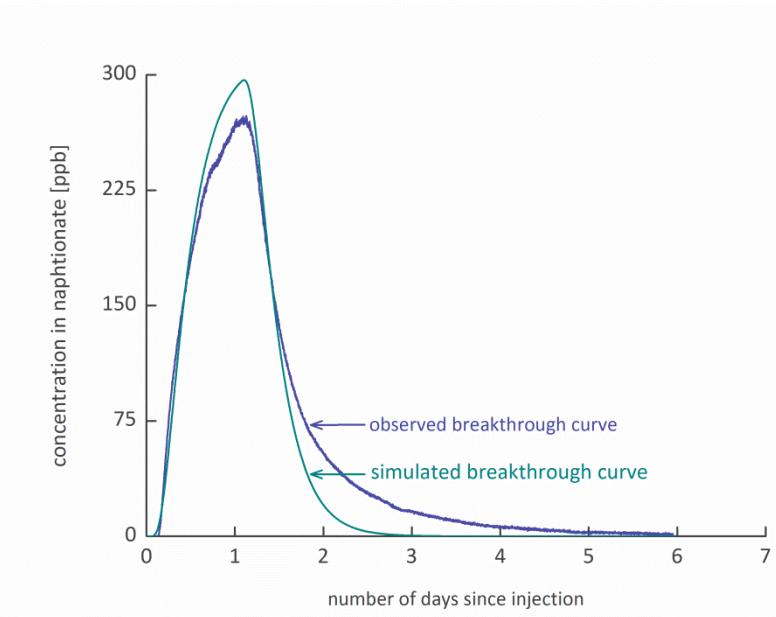
- Simultaneous injection of Heat and Fluorescent Dye
- Allowing to study different processes in the aquifer

- Injection in Pz9
- Monitoring in control panels
- Recovery at pumping well



2012 Thermal tracer test: Breakthrough curve at PP

- Radial converging flow



	Naphtionate	Temperature
Longitudinal dispersion (α_L) [m]	3	
Porosity (n) [-]	0.04	
1 st order degradation coefficient λ [s^{-1}]	1.5×10^{-5}	0
Retardation factor R [-]	1	5

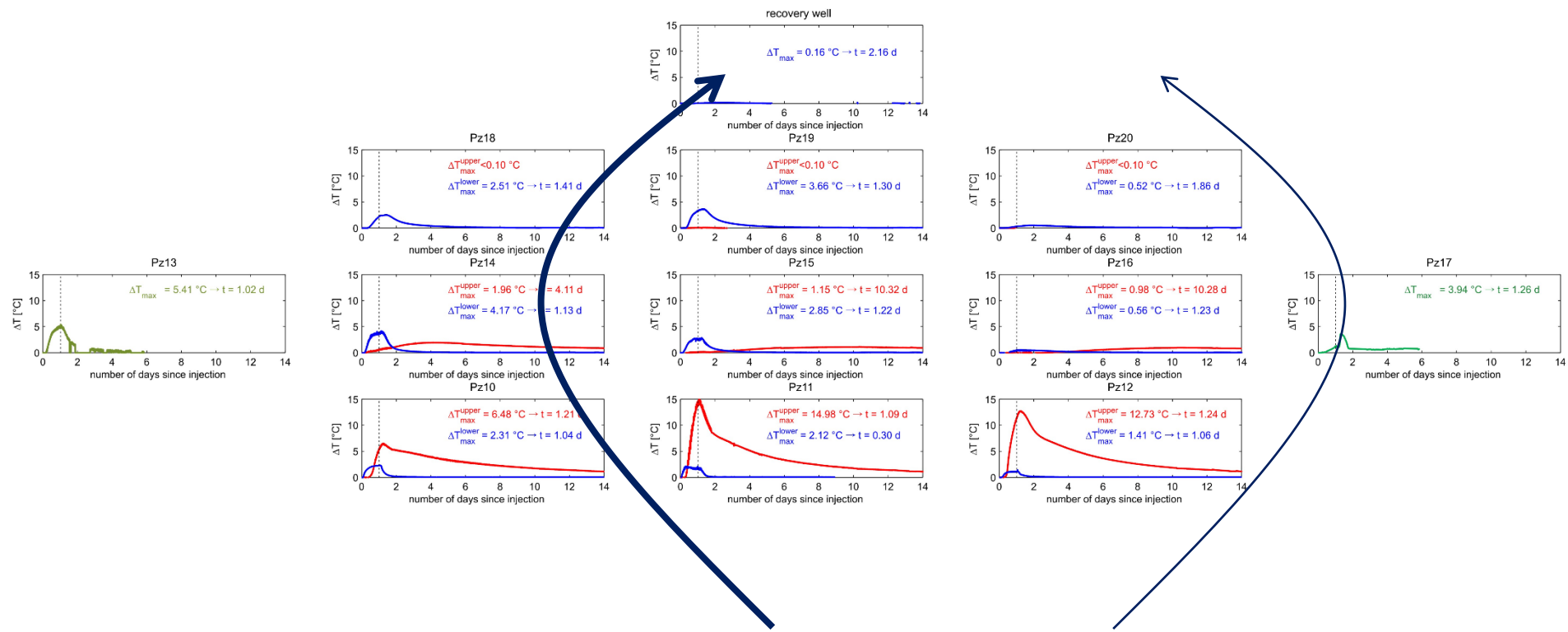
(Hecht-Méndez et al. 2010)

$$R = C_m / nC_w$$

$$C_m = 2.3 \text{ MJ/m}^3/\text{K}$$

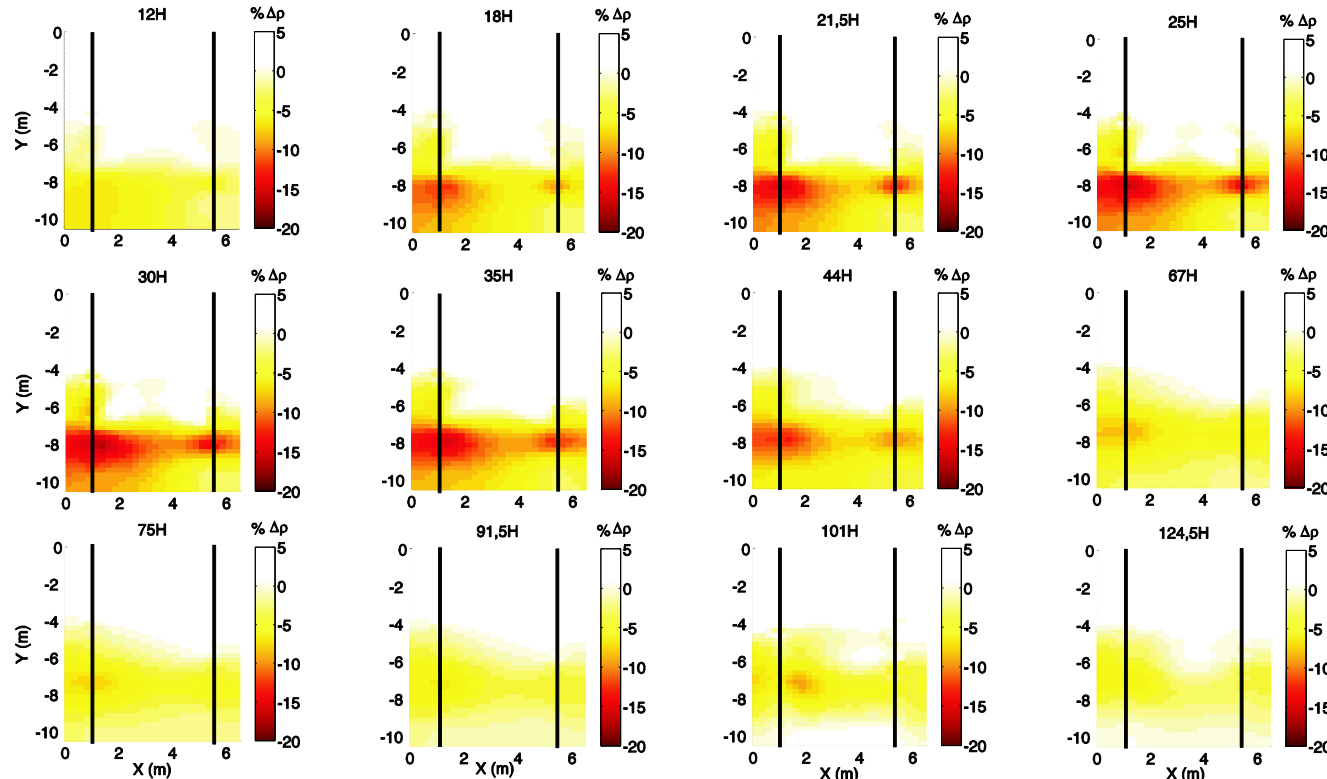
2012 Thermal tracer test: control panels T° curves

- Heterogeneity of the aquifer



Crosshole ERT: Spatial and temporal imaging of resistivity

- Lateral variations related to heterogeneity in the deposits
- Changes seem stronger around first borehole
- Spatially, temperatures increase only in the bottom part of the aquifer (clean gravel)
- Detection limit -3%



- Hermans, T. et al. (2015). Geothermics
<http://hdl.handle.net/2268/164949>

Measurement of GW flux and flow direction: FVPDM

Finite Volume Point Dilution Method

Generalisation of single well dilution techniques

Brouyère *et al.* 2008, J. Contam. Hydrol.

Pumping Well

- Darcy's flux in the
 - upper part of the aquifer 10 m/d
 - lower part of the aquifer 200 m/d

PzO2

-> **10 x times higher in the lower part**

- Measuring GW flow direction using an evolution of the FVPDM setup
- Diverging flow direction on the first control panel

× × × × ×

↖ ↗ ↖ ↘

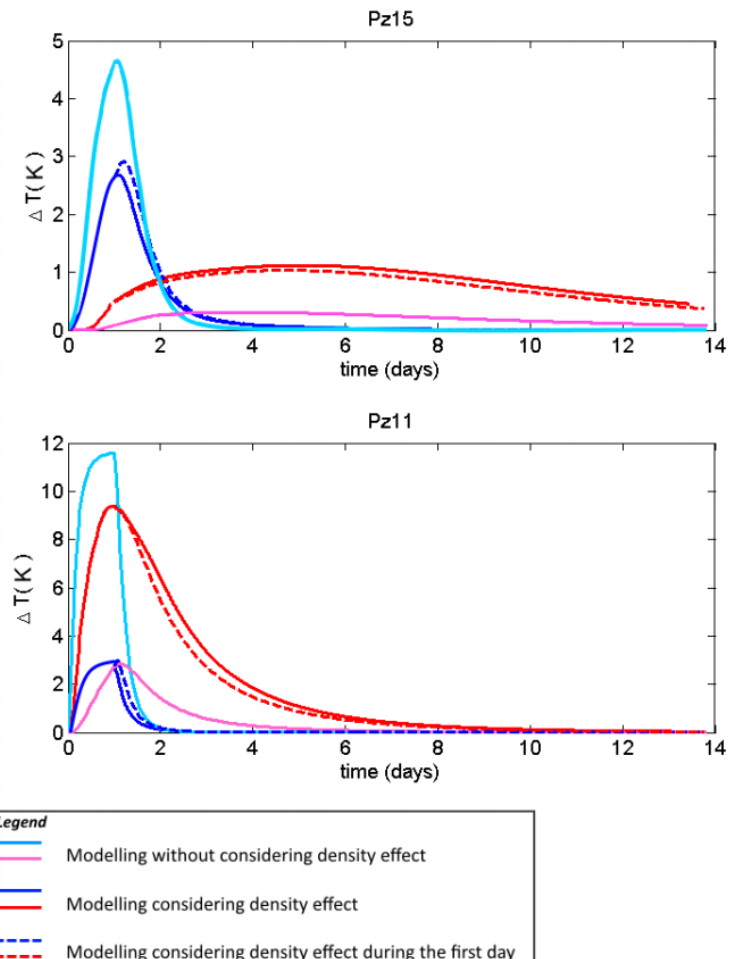
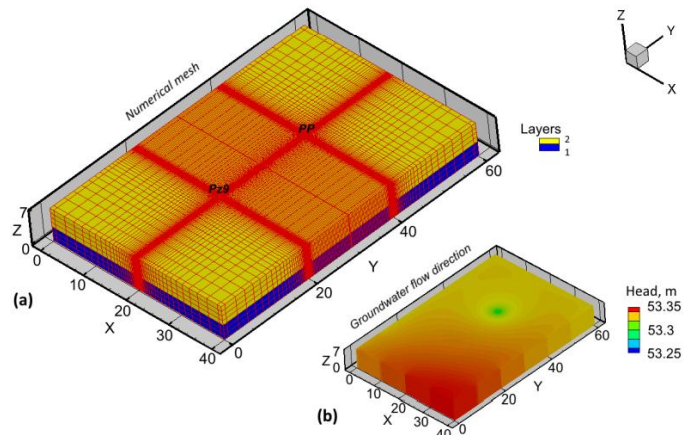
×

PzO9

↗ ↖

2015 Modeling of the 2012 thermal tracer test

- Modeling to study 3D shape of the heat plume (HGS)
- Calibration using T° bkth. curves and pilot points
- Complex behavior of the heat plume explained by high lateral and vertical heterogeneity of the hydraulic conductivity field
- Temperature-induced water density effect



Reference list

- Hermans, T., & Irving, J. (2017). Facies discrimination with electrical resistivity tomography using a probabilistic methodology: Effect of sensitivity and regularization. *Near Surface Geophysics*, 15, 13-25. <http://hdl.handle.net/2268/202474>
- Hermans T. et al. (2016). Covariance-constrained difference inversion of time-lapse electrical resistivity tomography data. *Geophysics*, 81(5), 311-E322. <http://hdl.handle.net/2268/197112>
- Klepikova M. et al. (2016). Heat tracer test in an alluvial aquifer: field experiment and inverse modelling. *Journal of hydrology*, 540, 812-823. <http://hdl.handle.net/2268/199598>
- Hermans, T. et al. (2016). Direct prediction of spatially and temporally varying physical properties from time-lapse electrical resistance data. *Water Resources Research*, 52, 7262-7283. <http://hdl.handle.net/2268/201489>
- Hermans, T. et al. (2015). Uncertainty in training image-based inversion of hydraulic head data constrained to ERT data: workflow and case study. *Water Resources Research*, 51, 5332-5352. <http://hdl.handle.net/2268/184023>
- Hermans, T. et al. (2015). Quantitative temperature monitoring of a heat tracing experiment using cross-borehole ERT. *Geothermics*, 53, 14-26. <http://hdl.handle.net/2268/164949>
- Hermans, T. (2014). Integration of near-surface geophysical, geological and hydrogeological data with multiple-point geostatistics in alluvial aquifers. PhD thesis, University of Liège. <http://hdl.handle.net/2268/163547>
- Wildemeersch S. et al. (2014). Coupling heat and chemical tracer experiments for estimating heat transfer parameters in shallow alluvial aquifers. *Journal of Contaminant Hydrology*, 169, 90-99. <http://hdl.handle.net/2268/171944>
- Brouyère S. (2001). Etude et modélisation du transport et du piégeage des solutés en milieu souterrain variablement saturé, PhD thesis, University of Liège. <http://bictel.ulg.ac.be/ETD-db/collection/available/ULgetd-08222007-101855/>